# Interplay of initial and final states for $(e,3e)$ and $(\gamma,2e)$ processes on helium

L. U. Ancarani,[1] G. Gasaneo,[2] F. D. Colavecchia,[3] and C. Dal Cappello[1]
[1]*Laboratoire de Physique Moléculaire et des Collisions, Université Paul Verlaine—Metz, 57078 Metz, France*
[2]*Departamento de Física, Universidad Nacional del Sur and Consejo Nacional de Investigaciones Científicas y Técnicas, 8000 Bahía Blanca, Buenos Aires, Argentina*
[3]*Centro Atómico Bariloche and Consejo Nacional de Investigaciones Científicas y Técnicas, 8400 S. C. de Bariloche, Río Negro, Argentina*
(Received 3 March 2008; published 20 June 2008)

The role of the description of initial and final states in $(\gamma,2e)$ and high incident energy $(e,3e)$ collisions with helium targets is investigated. We describe the double continuum as a product of plane waves modulated by three Coulomb distortion factors and propose different sets of initial states which satisfy exactly all two-body Kato cusp conditions. Wave functions with only angular correlation, and with both angular and radial correlation, are considered; in each case, the interparticle correlation factors are such that they have different (polynomial, exponentially increasing or decreasing, and oscillatory) asymptotic behaviors. The gauge discrepancies observed in $(\gamma,2e)$ calculations show that the overall agreement with absolute $(e,3e)$ experimental data at 10+10 eV ejected energy obtained with simple initial states is fortuitous and can hardly be attributed to a balanced description with respect to the final state. Thus the description of the final state by the product of plane waves and three Coulomb distortion factors is not suitable to describe sufficiently well the double continuum of two electrons ejected at 10 eV. An investigation of the ejected energy dependence on both double ionization processes further illustrates that what is observed at 10+10 eV ejected energy does not necessarily hold at higher values. Further theoretical studies and new experimental data are clearly needed to help understand the interplay of initial and final states.

DOI: 10.1103/PhysRevA.77.062712 PACS number(s): 34.80.Dp, 32.80.Fb

## I. INTRODUCTION

The theoretical study of the double ionization of helium, whether by electron [$(e,3e)$ experiments] [1] or photon [$(\gamma,2e)$ experiments] [2] impact, allows one to gain information on correlated systems. The full three-body Coulomb problem has been extensively studied, but no exact analytic wave function is known for either the scattering or the bound states. Hence approximate wave functions are used when calculating double ionization cross sections, and the choice of both the initial and final wave functions leads to different results (see below, and more generally Refs. [1,2]). In this paper, we wish to discuss this issue for both $(e,3e)$ and $(\gamma,2e)$ processes. One popular approximation of the final double continuum is given by the C3 wave function (also known as BBK) [5]. While it diagonalizes the three-body Hamiltonian and has the correct asymptotic behavior when all interparticle distances are large, it describes poorly the behavior at intermediate distances or when one particle is far away from the other two. That said, the C3 wave function is a very useful model; it has the advantage of being analytical so that it is practical to study ionization processes of a variety of atoms and molecules. Previous applications have shown that the C3 model can reproduce most of the observed cross sections' features, and, as with any approximate wave function, its validity can break down for some particular kinematical configurations. However, as we shall describe in more details below, the C3 double continuum is presently the model that leads to the best level of agreement, on the absolute scale, with the available high energy $(e,3e)$ experimental data where the two electrons escape with 10 eV each. In order to understand why this is so, we study in this contribution the interplay of the C3 final state with several initial bound state descriptions, not only for $(e,3e)$ but also for $(\gamma,2e)$ processes; the latter will allow us to confirm or not whether the "balanced" character of the approximated wave functions employed is responsible for the surprising good agreement for $(e,3e)$ processes.

The $(\gamma,2e)$ process is an excellent tool to study the correlation of two-electron systems since the double ionization process occurs only because of electron-electron correlation. The calculation of triple differential cross sections (TDCSs) can be performed in at least three different gauges [3], and the results are mathematically equal if the initial and final states wave functions employed are the solution of the same Hamiltonian. The gauge disagreement can thus be used as a measure of the differences on the initial and final Hamiltonians. A very careful and complete study of the gauge discrepancies on helium double photoionization (DPI) has been performed in the paper by Lucey *et al.* [4], where different approximate wave functions for two-electron systems presented in the literature have been tested. To represent the ejected electrons in the final channel, use was made of the double continuum C3 wave function and variants defined through the inclusion of effective charges. For the initial channel double bound wave functions with different degrees of accuracy were used including, e.g., the highly sophisticated approach of Kinoshita [6]. In all the cases tested gauge discrepancies were observed, leading to the following conclusion: if agreement between gauges is found, then (a) the initial and final state wave functions are the exact solutions of the three-body Hamiltonians, or (b) the approximated solutions used in the initial and final channel are solutions of the same approximated Hamiltonian. That said, the double continuum C3 wave function and very simple models for the

 

bound initial state, although sensitive to the chosen gauge, are able to describe accurately the main features of the experimental results for a variety of electron energy sharing conditions [4,7–9]. A study based on the convergent close-coupling (CCC) method was performed by Kheifets and Bray [10]. With a close-coupling approach the authors generate a highly correlated wave function for the final double continuum wave function and combine it with highly correlated 14- and 20-parameter Hylleraas-like wave functions for the initial channel. Their study showed that, when improving the quality of the initial wave function, agreement between gauges and with the experimental data can be found for different targets [10] including helium, and this up to high energy regimes. These authors reached thus the conclusion that the proposed wave functions can be considered as the solutions of the three body problems.

The double ionization of neutral atoms by electron impact, the $(e,3e)$ process, can also be used as a test of the correlation in two-electron systems. Absolute fivefold differential cross sections (FDCS) have been measured by Lahmam-Bennani *et al.* [11,12] for high incident energy and ejected energies of $E_1=E_2=4$ eV or $E_1=E_2=10$ eV (small momentum transfer). These measurements allow one to make a detailed study—both in shape and magnitude—of this double ionization process. On the theoretical side, there have been published calculations based on the CCC approach [12,13], the *J*-matrix method to Faddeev–Merkuriev differential equations [14,15], a wave-packet evolution approach [16], and the distorted wave approaches (with the "pure" C3 wave function [17–22] or variants with effective charges [11,23,24]). Since the experimental energy of the incoming projectile is high (5599 eV), the comparison between the theoretical calculations and the measured data can be performed within the frame of the first Born approximation (FBA) in the interaction of the projectile with the target atom; indeed, explicit second Born calculations showed that little difference is observed with either the CCC [25] or a distorted wave approach [26]. Even within the FBA, the FDCSs obtained with a different theoretical description of the initial and final states are not in agreement with each other, and yield a rather confusing picture. The results presented within the Born-CCC approach show an overall shape agreement but present important magnitude disagreements for both $E_1=E_2=4$ eV (factor 14 [12]) and $E_1=E_2=10$ eV (factor 3 [12] or 2.2 [13]) ejected energies. In Ref. [13], the authors applied different sets of initial state wave functions for both $(e,3e)$ and $(\gamma,2e)$ processes in the case $E_1=E_2=10$ eV. They showed that if functions which are less correlated than the 20-parameters Hylleraas function (like that of Le Sech [27] or of Pluvinage [28]) are used, gauge agreement is not found. Calculations with the *J*-matrix approach [14] (where the initial and final wave functions are represented by an infinite expansion in a Laguerre basis) yield a reasonable agreement in $(e,3e)$ cross sections magnitude, but to a lesser extent in their shapes. It should be noted that previously published calculations [15], where the pseudostates method was employed, showed important magnitude disagreements with experimental data, similarly to the CCC approach. Recently, a purely numerical calculation based on a wave-packet evolution approach yielded $(e,3e)$ cross sections which are close, in both shape and magnitude, to those found with the CCC approach. Finally, the calculations performed with distorted wave approaches lead to different and divergent conclusions. The combination of the C3 double continuum wave function for the ejected electrons with different double bound initial wave functions yields results which depend on the level of correlation included in the initial state. For $E_1=E_2=10$ eV ejected electron energies, agreement in shape, but disagreement in magnitude (factor 1.5–2) is found when comparing the calculation and the experimental data [11], when highly correlated double bound wave functions like that of Le Sech [27], Bonham and Kohl [29], or Hylleraas–like are used for the initial channel [18–20,26]. On the other hand, overall agreement in both shape and magnitude with the experimental data is found when the simple wave function proposed by Pluvinage is used [17]. The latter, although it is not the counterpart of the C3 double continuum [30], is constructed in a similar way since it is built as the product of three Coulomb wave functions and diagonalizes the three two-body Coulomb potentials. Practically the same agreement was observed by [18,21] using other simple wave functions (including the proper double bound version of the C3 function), which have a similar structure as Pluvinage's function. In all these studies, the different authors used what we shall call the "pure" C3 approach where use of effective charges was not considered (see comment in Sec. II C). For $E_1=E_2=4$ eV ejected energies, the C3 description of the double electron continuum is expected to be very poor, and indeed important magnitude disagreements are observed.

On the basis of the above $(\gamma,2e)$ and $(e,3e)$ results for ejected energies of $E_1=E_2=10$ eV, the following conclusions can be drawn: (1) approximations like the CCC which work well for the $(\gamma,2e)$ process do not seem to work as well for the $(e,3e)$ process; (2) highly correlated initial state wave functions in conjunction with the pure C3 model fail to describe the magnitude of the available high energy $(e,3e)$ absolute experimental cross sections; and (3) the combination of the C3 double continuum and simple approaches like the Pluvinage, or the C3 double bound functions, lead to the best agreement in both shape and magnitude for $(e,3e)$ cross sections. This last point has been attributed [19,31] to the fact that the used wave functions treat the interactions in the initial and final channels in a "balanced" way. One of the aims of this paper is to discuss this issue carefully.

In this paper we perform a systematic study of the cross sections for the double ionization of helium atoms, by both electron and photon impact in the same kinematical and geometrical situations. For $(e,3e)$ processes, the FDCSs are calculated within the FBA and the results are compared with the high energy absolute experimental data of Lahmam-Bennani *et al.* [11]. The two electrons ejected in the final channel at equal energy of $E_1=E_2=10$ eV are modeled with the "pure" C3 wave function, while different sets of double bound wave functions which depend on all the interparticle coordinates are proposed for the initial channel. In order to investigate the role (if any) played by different asymptotic behaviors in the electron-electron coordinate, we consider four different functional forms: exponentially decreasing, exponentially increasing, potentially divergent, and oscillatory behaviors. All

the wave functions considered satisfy exactly the two-body coalescence conditions, known as Kato cusp conditions [32], at the three two-body Coulomb divergencies. They are separated in classes depending on their mean energies, and the amount and the kind of correlation included. The comparison with the experimental data allows us to see which of them are balanced, for $(e,3e)$ processes, in the treatment of the interactions in the initial and final channel. The same set of initial and final channel wave functions are then used to evaluate the first-order Born triple differential cross sections for the $(\gamma,2e)$ process with the same kinematics. The comparison of the results obtained in the different gauges indicates whether the wave functions are really "balanced" or not. Next, we tackle the same issue but at higher escaping electrons energy $E_1=E_2$ to see whether the conclusions observed at 10 eV hold or not.

The rest of the paper is arranged as follows. In Sec. II, we introduce the definitions of the cross sections to be evaluated: for $(e,3e)$ processes, the fivefold differential cross section within the first Born approximation is given, and for $(\gamma,2e)$ the triple differential cross section is defined in the length, velocity, and acceleration forms. The double continuum C3 final state as well as all the double bound initial state wave functions considered are also presented in this section. The results of our calculations are presented in Sec. III and a summary and some perspectives are given in Sec. IV. Atomic units are used throughout ($\hbar=m_e=e=1$).

## II. THEORY

### A. $(e,3e)$

The fully differential cross section for the ejection of two electrons from a neutral atom by electron impact, the $(e,3e)$ reaction, is given by

$$\frac{d^5\sigma}{d\Omega_0 d\Omega_1 d\Omega_2 dE_1 dE_2} = (2\pi)^4 \frac{k_0 k_1 k_2}{k_i} |T_{fi}(\mathbf{k}_0,\mathbf{k}_1,\mathbf{k}_2)|^2. \quad (1)$$

Here $\mathbf{k}_i$ and $\mathbf{k}_0$ are the momenta of the incoming and outgoing projectile, $\mathbf{k}_1$ and $\mathbf{k}_2$ are the momenta of the ejected electrons after the collision (energy $E_1,E_2$); $d\Omega_0$, $d\Omega_1$, and $d\Omega_2$ denote, respectively, the solid angle elements for the scattered and the two ejected electrons. We shall restrict the present investigation to high incident energies, so that the FBA for the transition matrix $T_{fi}$ may be taken

$$T_{fi} = \left\langle \frac{1}{(2\pi)^{3/2}} e^{i\mathbf{k}_0\cdot\mathbf{r}_0} \Psi_f^-(\mathbf{r}_1,\mathbf{r}_2) \middle| -\frac{Z}{r_0} + \frac{1}{r_{01}} + \frac{1}{r_{02}} \middle| \frac{1}{(2\pi)^{3/2}} e^{i\mathbf{k}_i\cdot\mathbf{r}_0} \Psi_i(\mathbf{r}_1,\mathbf{r}_2) \right\rangle, \quad (2)$$

where $Z=2$ is the helium nuclear charge. Here $\Psi_i(\mathbf{r}_1,\mathbf{r}_2)$ and $\Psi_f^-(\mathbf{r}_1,\mathbf{r}_2)$ are the exact initial and final channel wave functions for the two-electron system under consideration. The integration over the projectile coordinates $(\mathbf{r}_0)$ can be performed analytically so that the transition amplitude reduces to

$$T_{fi} = \frac{1}{2\pi^2 q^2} \langle \Psi_f^-(\mathbf{r}_1,\mathbf{r}_2) | -Z + e^{i\mathbf{q}\cdot\mathbf{r}_1} + e^{i\mathbf{q}\cdot\mathbf{r}_2} | \Psi_i(\mathbf{r}_1,\mathbf{r}_2) \rangle, \quad (3)$$

where $\mathbf{q}=\mathbf{k}_i-\mathbf{k}_0$ is the momentum transferred from the projectile to the target atom.

The integration is numerically performed as indicated in Sec. II of Ref. [18]. Briefly, the calculation reduces to a sum of double numerical integrations for initial wave functions containing exponential and powers of the coordinates, and to a sum of three-dimensional integrations when Pluvinage-type wave functions are considered.

### B. $(\gamma,2e)$

Since the double photoionization of atomic species by single photons occurs only due to the electron-electron correlation, it is a very convenient process to probe the role of this correlation in different initial states. Moreover, one of the most important advantages over other collisional processes involving charged particles is that there is no long-range interaction between the target and the incoming particle. Since most of the experimental DPI data have been collected in collisions of incident photons with small momenta, we assume a dipolar approximation for the process.

The triply differential cross section in terms of the momenta $\mathbf{k}_1$ and $\mathbf{k}_2$ of the two ejected electrons is given by

$$\frac{d\sigma}{d\Omega_1 d\Omega_2 dE_2} = 4\pi^2 \alpha k_1 k_2 C^{(G)} |T^{(G)}(\mathbf{k}_1,\mathbf{k}_2)|^2 \quad (4)$$

and can be computed in different *gauges*, represented by the superscript $(G)$; $\alpha$ is the fine structure constant. Writing the transition matrix as

$$T^{(G)}(\mathbf{k}_1,\mathbf{k}_2) = \langle \Psi_f^-(\mathbf{r}_1,\mathbf{r}_2) | W^{(G)}(\mathbf{r}_1,\mathbf{r}_2) | \Psi_i(\mathbf{r}_1,\mathbf{r}_2) \rangle, \quad (5)$$

the acceleration $(A)$, velocity $(V)$, and length $(L)$ forms of the perturbation are

$$W^{(A)}(\mathbf{r}_1,\mathbf{r}_2) = \boldsymbol{\varepsilon}\cdot\left(\frac{\mathbf{r}_1}{r_1^3} + \frac{\mathbf{r}_2}{r_2^3}\right),$$

$$W^{(V)}(\mathbf{r}_1,\mathbf{r}_2) = \boldsymbol{\varepsilon}\cdot(\boldsymbol{\nabla}_1 + \boldsymbol{\nabla}_2),$$

$$W^{(L)}(\mathbf{r}_1,\mathbf{r}_2) = \boldsymbol{\varepsilon}\cdot(\mathbf{r}_1 + \mathbf{r}_2),$$

where $\boldsymbol{\varepsilon}$ is the polarization vector of the incoming photon. The normalization constants for each gauge are

$$C^{(A)} = Z^2/\omega^3,$$

$$C^{(V)} = 1/\omega,$$

$$C^{(L)} = \omega,$$

where $\omega$ is the angular frequency of the incoming photon. In the transition matrix, Eq. (5), the wave functions $\Psi_i(\mathbf{r}_1,\mathbf{r}_2)$ and $\Psi_f^-(\mathbf{r}_1,\mathbf{r}_2)$ are the same as those used in Eq. (2).

We recall that each of the three different gauges gives a particular emphasis to different parts of the configuration

space, namely the small (acceleration form), intermediate (velocity form), or large (length form) distances from the nucleus. The theoretical description of the process with wave functions, initial and final, which do not satisfy exactly the same Schrödinger equation yield gauge dependent results. Thus even when approximated wave functions for the two-electron initial and final channels are used, they should be solutions of the same Hamiltonian, or at least treated with the same level of approximation; otherwise, discrepancies between gauges are observed [4,10].

The calculation of $T^{(G)}(\mathbf{k}_1,\mathbf{k}_2)$ is performed by direct six-dimensional numerical integration in the spherical representation of coordinates $\mathbf{r}_1$ and $\mathbf{r}_2$ using a nondeterministic Vegas algorithm. The relative error of the TDCS is less than 3% for all energies and angles considered in Sec. III.

### C. Final state

The dynamics of the two escaping electrons is represented here, for both $(e,3e)$ and $(\gamma,2e)$ processes, by a symmetrized C3 (or BBK) wave function [5]

$$\Psi_f^-(\mathbf{r}_1,\mathbf{r}_2)=\Psi_{C3}^-(\mathbf{r}_1,\mathbf{r}_2)=\psi_{\mathbf{k}_1}^-(\mathbf{r}_1)\psi_{\mathbf{k}_2}^-(\mathbf{r}_2)D^-(\alpha_{12},\mathbf{k}_{12},\mathbf{r}_{12}). \tag{6}$$

In this model the electron-nucleus interactions are described by the two-body Coulomb functions $\psi_{\mathbf{k}_i}^-(\mathbf{r}_i)$, while the electron-electron correlation by a Coulomb distortion factor $D^-(\alpha_{12},\mathbf{k}_{12},\mathbf{r}_{12})={}_1F_1[i\alpha_{12},1,-i(k_{12}r_{12}+\mathbf{k}_{12}\cdot\mathbf{r}_{12})]$, where $\alpha_{12}=1/(2k_{12})$ and the relative momentum $\mathbf{k}_{12}=(\mathbf{k}_1-\mathbf{k}_2)/2$. As is well-known, the C3 function diagonalizes all three Coulomb interactions, and hence satisfies exactly Kato two-body cusp conditions. Moreover, the C3 double continuum has the correct asymptotic behavior when all interparticle distances are large. Not all kinematical terms of the three-body Hamiltonian, however, are solved by this function [30]. Correlation in the three-body problem can be measured by comparing the full three-body solution with the independent particle model (IPM) [3], given in the case of the double continuum by the C2 approach: $\Psi_{C2}^-(\mathbf{r}_1,\mathbf{r}_2)=\psi_{\mathbf{k}_1}^-(\mathbf{r}_1)\psi_{\mathbf{k}_2}^-(\mathbf{r}_2)$. It is then clear from the definition of $\Psi_{C3}^-(\mathbf{r}_1,\mathbf{r}_2)$ that the only piece of correlation included by the model is given by the Coulomb distortion factor $D^-(\alpha_{12},\mathbf{k}_{12},\mathbf{r}_{12})$ which depends purely on the $\mathbf{r}_{12}$ coordinate, and not (explicitly) on the $\mathbf{r}_1$ or $\mathbf{r}_2$ coordinates (the only dependence on $\mathbf{r}_1$ and $\mathbf{r}_2$ is indirect, through $\mathbf{r}_{12}$).

In this paper we have opted not to use variants of the C3 wave function with effective charges, position- or velocity-dependent Sommerfeld parameters (or highly correlated wave functions like those of Refs. [33,34]). Many different sets of them have been introduced in the literature (see, e.g., [1]), but none of them is accurate, that is to say, equivalent, for all kinematic conditions (the choice of effective charges is arbitrary, and the improvement with respect to the pure C3 wave function is highly dependent on the kinematical conditions of the double ionization process under scrutiny).

The exact double-continuum state $\Psi_f^-(\mathbf{r}_1,\mathbf{r}_2)$ and the initial ground state $\Psi_i(\mathbf{r}_1,\mathbf{r}_2)$ are orthogonal because they are solutions of the same three-body Hamiltonian. However, since the final state $\Psi_{C3}^-$ and the initial states introduced in the next section are only approximate solutions, they are not orthogonal. For that reason we may enforce their orthogonality by using the following definition for the final state wave function:

$$\langle\Psi_f^{-\perp}|=\langle\Psi_f^-|-\langle\Psi_f^-|\Psi_i\rangle\langle\Psi_i|.$$

For the $(e,3e)$ processes under scrutiny here, this operation does not affect much the shapes of the cross sections but gives a magnitude change of 10%–15% depending on the ejected angles [18]. In the case of DPI, this orthogonalization has no effect because of symmetry.

### D. Initial helium bound states

A great amount of ground state wave functions for the helium atom have been presented in the literature, and many different type of constructions have been used to approximately include the correlation. Here we make a selection of them and built some others in order to investigate separately the roles of the mean energy value and of the functional form of the correlation on the description of $(\gamma,2e)$ and $(e,3e)$ cross sections. Among these, we shall consider only trial wave functions which satisfy exactly all Kato cusp conditions [32] at the two-body coalescence points, that is to say functions which deal exactly with the three Coulomb singularities.

We shall subdivide the selected trial wave functions in three classes according to the amount of correlation included, measured with respect to the IPM. Here, we define *angular correlation* as the amount of correlation included by factors which depend only on the interparticle coordinate $\mathbf{r}_{12}$ while *radial correlation* is due to any other presence of the coordinates $\mathbf{r}_1$ and $\mathbf{r}_2$ in the wave function. Each class will be characterized by practically the same ground state mean energy and contains correlated wave functions which: (1) have only angular correlation (label *A*) and with energies close to saturation; (2) are obtained using the *angular correlated configuration interaction* [35,36] and include a limited amount of both radial and angular correlation (label AR); and (3) are obtained using more advanced approaches (label MA) to include radial and angular correlation with a faster convergency rate on the mean energy. To test how the trial functions are balanced with respect to the double continuum C3 wave function, four different asymptotic behaviors in the interelectronic coordinate $r_{12}$ are explored within each of the mentioned classes: exponentially decreasing (label $e-$), exponentially increasing (label $e+$), potentially divergent (label *P*), and oscillatory behavior (label *Os*). Moreover, we shall use the following compact notation: $1s=e^{-Zr}$ and $2s=e^{-Zr/2}(1-\frac{Z}{2}r)$, so that, for example, the term $1s1s$ will represent the function $e^{-Z(r_1+r_2)}$ and $1s2s$ the function $e^{-Z(r_1+r_2/2)}(1-\frac{Z}{2}r_2)$.

#### 1. $\psi_i$ with angular correlation only (*A*)

First, we consider trial wave functions which contain angular correlation only. By this we mean the product of two ground state hydrogenic functions $1s1s$ multiplied by an angular correlation function which depends only on the inter-

electronic distance $r_{12}$. Depending on the functional form of this factor, four trial wave functions are proposed. They all yield a similar ground state energy of about $E=-2.879$ a.u. (Note that this is slightly off the best energy $E=-2.8793$ a.u.—saturation energy—that can be obtained with such class of function [23,35].)

*Polynomial.* To obtain a polynomial correlation factor we use the recently proposed C3-like basis functions [35]. One such function is given by

$$\Psi^{A,P} = N^{A.P} 1s1s\left[1 + \frac{r_{12}}{2} + 0.038\ 89\ \ r_{12}^2\right],$$

$$N^{A.P} = 1.553\ 14,$$

$$E^{A.P} = -2.8785\ \ \text{a.u.} \tag{7}$$

At large $r_{12}$ values, the correlation factor increases as a second order polynomial.

*Decreasing to one exponentially.* The following function

$$\Psi^{A,e-} = N^{A,e-} 1s1s\left[1 + \frac{r_{12}}{2}(1 + 0.0995 r_{12}) e^{-0.0145 r_{12}}\right],$$

$$N^{A,e-} = 1.549\ 04,$$

$$E^{A,e-} = -2.8785\ \ \text{a.u.} \tag{8}$$

has an angular correlation factor which tends to one exponentially at large interelectronic distances, though rather slowly.

*Increasing exponentially.* Next, we consider a correlation factor which grows exponentially at large interparticle distances,

$$\Psi^{A,e+} = N^{A,e+} 1s1s\left[1 + \frac{1}{2} r_{12} e^{0.074 r_{12}}\right],$$

$$N^{A,e+} = 1.551\ 98,$$

$$E^{A,e+} = -2.8786\ \ \text{a.u.} \tag{9}$$

*Oscillating and going to zero.* Finally, we consider Pluvinage's wave function [28] which has a different behavior since the correlation factor oscillates and tends to zero, but very slowly, at large $r_{12}$ values. For helium, it reads

$$\Psi^{A,Os} = \Psi^{B}_{PLU}(1,1,\kappa) = N^{B}_{PLU}(1,1,\kappa) 1s1s \times e^{-i\kappa r_{12}} {}_1F_1\left(1 - \frac{i}{2\kappa}, 2, 2i\kappa r_{12}\right),$$

$$N^{B}_{PLU}(1,1,0.41) = 1.5365,$$

$$E^{A,Os} = -2.8781\ \ \text{a.u.}, \tag{10}$$

where the optimized parameter is $\kappa=0.41$. Note that this correlation function has unphysical nodes [18].

### 2. $\psi_i$ with angular and radial correlation: Configuration interaction (AR)

We now consider trial wave functions which include a limited amount of both radial and angular correlation constructed with the *angular correlated configuration interaction* method. In all cases described below, the functions are built with a superposition of the $1s1s$ and $1s2s+2s1s$ configurations, and are such that the Kato cusp conditions at all the two-body coalescence are satisfied. The angular correlation factors are introduced either *ad hoc* or through the use of specific basis functions, the C3-like [35] or Pluvinage-like [22] (these are built as a product of three factors: two Coulomb wave functions for the electron-nucleus interaction and a distortion factor depending purely on the interelectronic coordinate). The following trial wave functions yield a similar ground state energy of about $E=-2.894$ a.u.

*Polynomial.* To obtain a polynomial correlation factor we take again one of the recently proposed [35] C3-like trial wave functions, built with C3-like basis functions which, by construction, diagonalize all the Coulomb interactions. The function reads

$$\psi^{AR,P} = N^{AR,P}\left[1s1s\left(1 + \frac{r_{12}}{2} - 0.028\ 154 r_{12}^2\right) - 0.043\ 788(1s2s + 2s1s)\left(1 + \frac{r_{12}}{2} - 0.111\ 040 r_{12}^2\right)\right],$$

$$N^{AR,P} = 1.622\ 80,$$

$$E^{AR,P} = -2.8951\ \ \text{a.u.} \tag{11}$$

*Decreasing to one exponentially.* Next we use two *ad hoc* correlation factors which tend to one at large $r_{12}$ and represent the screening produced by the nucleus over the bound electrons

$$\psi^{AR,e-} = N^{AR,e-}\left[1s1s\left(1 - \frac{e^{-\beta r_{12}}}{2\beta + 1}\right) - 0.0146(1s2s + 2s1s)\left(1 - \frac{e^{-\gamma r_{12}}}{2\gamma + 1}\right)\right],$$

$$\beta = 0.151, \quad \gamma = 3.6,$$

$$N^{AR,e-} = 7.067\ 769,$$

$$E^{AR,e-} = -2.8947\ \ \text{a.u.} \tag{12}$$

*Increasing exponentially.* Next, we construct a trial wave function which has correlation factors which grow exponentially at large $r_{12}$,

$$\psi^{AR,e+} = N^{AR,e+}[1s1s(1 - 1.031\ 45 e^{\beta r_{12}}) + 0.026\ 163 \times (1s2s + 2s1s)(1 - 0.555 e^{-\gamma r_{12}} - 0.396\ 29 e^{\delta r_{12}})],$$

$$\beta = 0.015\ 25, \quad \gamma = 0.116, \quad \delta = 0.101,$$

$$N^{AR,e+} = 49.913,$$

$$E^{AR,e+} = -2.8941 \text{ a.u.} \tag{13}$$

*Oscillating and going to zero.* Finally, using the Pluvinage-like basis set with oscillating Coulomb functions, the following wave function was proposed [22]:

$$\Psi^{AR,Os} = N^{AR,Os}\left\{1s1s\ \ e^{-i\kappa_{11}r_{12}}{}_1F_1\left[1-\frac{i}{2\kappa_{11}},2,2i\kappa_{11}r_{12}\right]\right.$$
$$-0.050(1s2s+2s1s)$$
$$\left.\times e^{-i\kappa_{12}r_{12}}{}_1F_1\left[1-\frac{i}{2\kappa_{12}},2,2i\kappa_{12}r_{12}\right]\right\},$$

$$\kappa_{11}=0.600, \quad \kappa_{12}=0.900,$$

$$N^{AR,Os}=1.5816,$$

$$E^{AR,Os}=-2.894 \text{ a.u.} \tag{14}$$

It suffers from the same problem as the original Pluvinage wave function, since it has unphysical nodes produced by the zeros of the Coulomb functions.

#### 3. $\psi_i$ with angular and radial correlation: More advanced functions (MA)

In this section we present what we shall call more advanced functions, which yield practically the same rather good mean energy of about $E=-2.902$ a.u. As we could not encounter a relatively simple trial wave function with a Pluvinage-type oscillatory behavior, we shall limit the study here to polynomial and exponential behaviors.

*Polynomial (Hylleraas type).* First we consider a function having a polynomial behavior where all interelectronic coordinates appear,

$$\Psi^{MA,P} = N^{MA,P}1s1s\left\{\left(1+\frac{r_{12}}{2}\right)[1+0.112\ 166(r_1^2+r_2^2)\right.$$
$$+0.020\ 637\ 3(r_1^3+r_2^3)]-0.078\ 078\ 2\ \ r_{12}^2[1$$
$$\left.+0.167\ 514(r_1^2+r_2^2)-0.015\ 235\ 2(r_1^3+r_2^3)]\right\},$$

$$N^{MA,P}=1.40001,$$

$$E^{MA,P}=-2.9020 \text{ a.u.} \tag{15}$$

This Hylleraas-type wave function is built using the *angular correlated configuration interaction* method discussed in Ref. [36]. and the C3-type basis set [35]. Correlation, in addition to the one included by the basis set, is included in the wave function by multiplying each C3-type configuration by a factor which has radial correlation.

*Exponential decreasing.* A function with exponentially decreasing behavior on the $r_{12}$ coordinate have been given by Le Sech [27]:

$$\Psi^{MA,e-}=\Psi_{LS}=N_{LS}\ \ 1s1s[\cosh(\lambda r_1)+\cosh(\lambda r_2)]$$
$$\times\left(1+\frac{1}{2}r_{12}e^{-ar_{12}}\right),$$

$$\lambda=0.7, \quad a=0.17,$$

$$N^{MA,e-}=N_{LS}=0.702\ 053\ 4,$$

$$E^{MA,e-}=E_{LS}=-2.9020 \text{ a.u.} \tag{16}$$

The angular correlation of this wave functions differs from that of $\Psi^{MA,P}$ in the large $r_{12}$ behavior, since angular correlation dies out in $\Psi_{LS}$ and not in $\Psi^{MA,P}$. Note also that the LS function contains radial correlation through the presence of a screening factor given by the $\cosh(\lambda r_i)$.

*Exponential increasing.* For an exponentially growing behavior at large $r_{12}$ distances, we propose a function similar to that given by Le Sech, but with a modified correlation factor

$$\Psi^{MA,e+} = N^{MA,e^+}1s1s[\cosh(\lambda r_1)+\cosh(\lambda r_2)]$$
$$\times\left(1+\frac{1}{2}r_{12}e^{-ar_{12}}-0.002\ 618r_{12}^2e^{br_{12}}\right),$$

$$\lambda=0.725\ 333, \quad a=0.190\ 54, \quad b=0.15,$$

$$N^{MA,e^+}=0.701\ 189,$$

$$E^{MA,e^+}=-2.9020 \text{ a.u.} \tag{17}$$

#### 4. Mean values

Table I displays the mean values of the ground state energy and of several radial and angular quantities obtained with each of the double bound wave functions given above. By comparison with the *numerically exact* values given by Drake [37], these quantities allow one to assess on the quality of each wave functions in different regions of the configuration space. We can see how the different mean values are gradually improved when more and more correlation is added into the trial wave functions. For the functions having angular correlation only ($A$), the mean values (including the energy) are close to the saturation values (not given here) which can be obtained within this class of functions [21,23,35]. The more advanced functions (MA) yield mean values which, in most cases, agree up to the third significant figure when compared to the *numerically exact* values. The results, presented here, obtained with the configuration interaction-type of construction (AR) can be considered as of intermediate quality. Although it is not the purpose here, these AR functions can be easily improved by adding more $nsn's$ terms; if a sufficient number of them are included, convergence toward the MA results can be achieved (see, e.g., [35]).

## III. RESULTS

To study the role played by the initial bound wave function, we have calculated cross sections for both $(\gamma,2e)$ and $(e,3e)$ processes on the ground state of helium, in the same kinematical and geometrical conditions. We shall present the results in two sections: the first one (Sec. III A) is those obtained in the kinematics of the only absolute $(e,3e)$ ex-

TABLE I. Energies and mean values for the trial wave functions presented in the text. Numerically exact values were taken from Drake [37].

| Trial function | Equation | $-\langle E\rangle$ | $\langle r_i\rangle$ | $\langle r_i^2\rangle$ | $\langle 1/r_i\rangle$ | $\langle r_{12}\rangle$ | $\langle r_{12}^2\rangle$ | $\langle 1/r_{12}\rangle$ | $\langle \hat{\mathbf{r}}_1\cdot\hat{\mathbf{r}}_2\rangle$ |
|---|---|---|---|---|---|---|---|---|---|
| $\Psi^{A,P}$ | (7) | 2.8785 | 0.8613 | 0.9951 | 1.7665 | 1.3385 | 2.2057 | 0.9934 | −0.1168 |
| $\Psi^{A,e-}$ | (8) | 2.8785 | 0.8620 | 0.9968 | 1.7650 | 1.3401 | 2.2106 | 0.9920 | −0.1175 |
| $\Psi^{A,e+}$ | (9) | 2.8786 | 0.8623 | 0.9981 | 1.7650 | 1.3407 | 2.2146 | 0.9923 | −0.1175 |
| $\Psi^{A,Os}$ | (10) | 2.8781 | 0.8633 | 0.9988 | 1.7615 | 1.3430 | 2.2161 | 0.9882 | −0.1192 |
| $\Psi^{AR,P}$ | (11) | 2.8951 | 0.9237 | 1.2141 | 1.7160 | 1.4249 | 2.5679 | 0.9543 | −0.0834 |
| $\Psi^{AR,e-}$ | (12) | 2.8947 | 0.9288 | 1.2473 | 1.7140 | 1.4350 | 2.6430 | 0.9526 | −0.0839 |
| $\Psi^{AR,e+}$ | (13) | 2.8941 | 0.9279 | 1.2151 | 1.7019 | 1.4399 | 2.6068 | 0.9403 | −0.0976 |
| $\Psi^{AR,Os}$ | (14) | 2.8940 | 0.9229 | 1.1839 | 1.7025 | 1.4213 | 2.4935 | 0.9410 | −0.0855 |
| $\Psi^{MA,P}$ | (15) | 2.9020 | 0.9318 | 1.1991 | 1.6815 | 1.4211 | 2.5135 | 0.9464 | −0.0652 |
| $\Psi^{MA,e-}$ | (16) | 2.9020 | 0.9312 | 1.1988 | 1.6811 | 1.4239 | 2.5303 | 0.9466 | −0.0664 |
| $\Psi^{MA,e+}$ | (17) | 2.9020 | 0.9321 | 1.2016 | 1.6805 | 1.4213 | 2.5195 | 0.9480 | −0.0647 |
| Exact | | 2.9037 | 0.9295 | 1.1935 | 1.6883 | 1.4221 | 2.5164 | 0.9458 | −0.0647 |

perimental data [11] where the two electrons escape with equal energy of $E_1=E_2=10$ eV; in the second (Sec. III B) we shall vary the ejected electrons' energy $E_1=E_2$.

### A. $E_1=E_2=10$ eV

Let us start with the kinematics used in the only absolute $(e,3e)$ measurement [11] with an incident energy of ~5.6 keV and two ejected electrons detected with equal energy (10 eV). In the coplanar $(e,3e)$ experiment, the projectile's scattering angle was 0.45°, and cross sections were measured at 20 angles $\theta_1$ of one of the ejected electrons as a function of the angle $\theta_2$ of the other ejected electron (all angles are measured in the same sense with respect to the incident beam direction).

For $(e,3e)$ processes, our calculated FDCSs are plotted in Fig. 1 as a function of the angle $\theta_2$ of one of the ejected electrons. For illustration purposes, we have selected the two ejected angles $\theta_1$ which correspond to the direction of the momentum transfer $\theta_1=319°$ and its opposite $\theta_1=139°$; similar results are found for 16 out of 20 geometrical situations presented in Ref. [11]. For each case, the three panels correspond to the three classes ($A$, AR, MA) of initial bound states. To optimize the visual comparison, the same scale (in a.u.) is used for each angle $\theta_1$. A first observation shows that shapes of the cross sections are rather well-reproduced with most bound trial wave functions; however, magnitude agreement is obtained only when pure angular correlation ($A$) is included [17,18,21].

For $(\gamma,2e)$ processes the TDCSs were calculated in all gauges for the same outgoing kinematical and geometrical situations as in Fig. 1, but with the polarization vector along the direction 0°. In Fig. 2, the velocity gauge ($V$) results for $\theta_1=139°$ are shown on a relative scale where all cross sections are normalized to one at the maximum. Note that, because of symmetry, the calculated cross sections for $\theta_1=319°$ are just the same but simply shifted by 180° in $\theta_2$. Since the initial and final states used in the calculations are not the solution of the same Hamiltonian, important gauge discrepancies are observed in all cases. To define a quantity that describes these discrepancies we have computed, for each kinematical condition, the ratios of the TDCSs at the maximum calculated in different gauges,

$$L/V=\frac{\max(\mathrm{TDCS}^{(L)})}{\max(\mathrm{TDCS}^{(V)})},$$

$$L/A=\frac{\max(\mathrm{TDCS}^{(L)})}{\max(\mathrm{TDCS}^{(A)})}. \tag{18}$$

For illustration, the ratios computed for $\theta_1=139°$ are shown in Table II (similar findings are observed for other angles). This enables us to compare the relative magnitude of the cross sections for the different initial states considered, and the importance of the gauge discrepancies. Overall the magnitude of the discrepancies is similar to those found by Lucey *et al.* [4] using the C3 double continuum and different sets of initial state wave functions.

#### 1. $\psi_i$ with angular correlation only ($A$)

All trial wave functions with angular correlation only (see top panel of Fig. 1) give practically the same $(e,3e)$ results (curves almost indistinguishable) and a satisfactory agreement with experimental data, in both shape and magnitude. The agreement does not seem to be related to the functional form of the correlation factor, including the oscillating behavior of the Pluvinage wave function. In Ref. [18] it has further been observed that other initial bound states with similar energy values, but which do not satisfy Kato cusp conditions, also yield the same kind of cross sections. Hence wave functions with angular correlation only, respecting or not Kato cusp conditions, are able to reproduce satisfactorily the available experimental data.

For $(\gamma,2e)$, all functions give again roughly the same TDCS shapes (indistinguishable in the figure), except for the relative amplitude of the secondary peak in the case of Pluvinage's oscillatory bound state. Important gauge discrepancies are observed (see the ratios $L/V$ and $L/A$ in Table II), but are

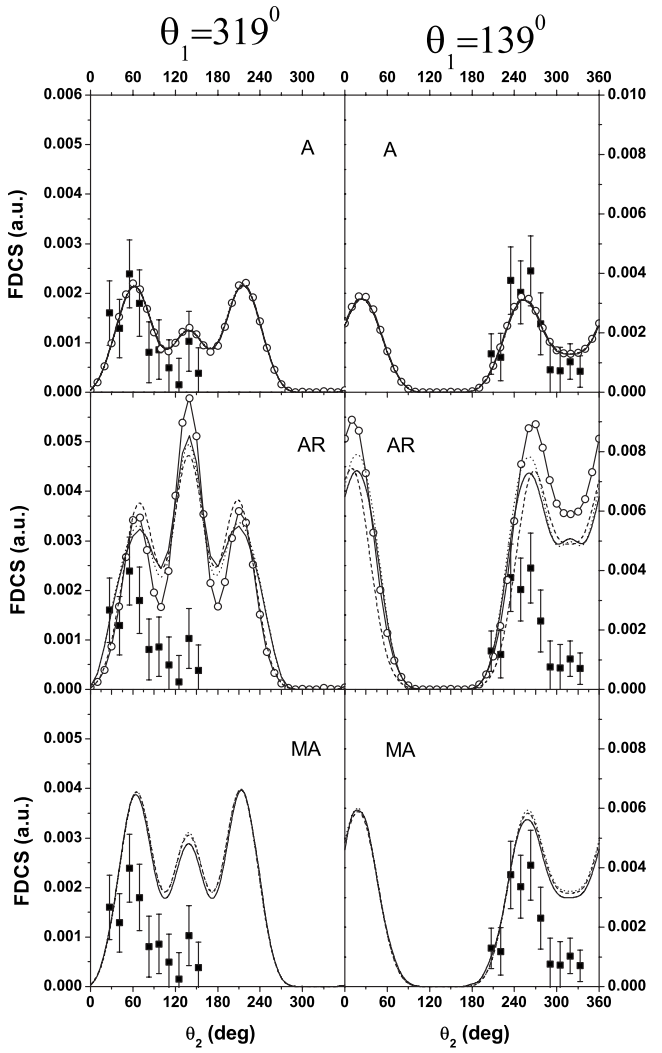


FIG. 1. Fivefold differential cross section (FDCS) for $(e,3e)$ ionization of the helium ground state, as a function of the angle of one of the ejected electrons $\theta_2$, with $\theta_1$ fixed as indicated. The incident electron (at ~5.6 keV) is scattered at 0.45°, and the two ejected electrons escape with equal energy (10 eV). The absolute experimental data [11]: full squares. The calculated FDCSs are obtained with the C3 final state and several initial state wave functions: top panel, *A* functions; middle panel, AR functions; and bottom panel, MA functions. In all panels, functions with polynomial behavior are plotted with solid lines, those with exponentially decreasing behavior with dashed lines, those with exponentially increasing behavior with dotted lines, and with oscillatory conditions with solid lines with open circles.

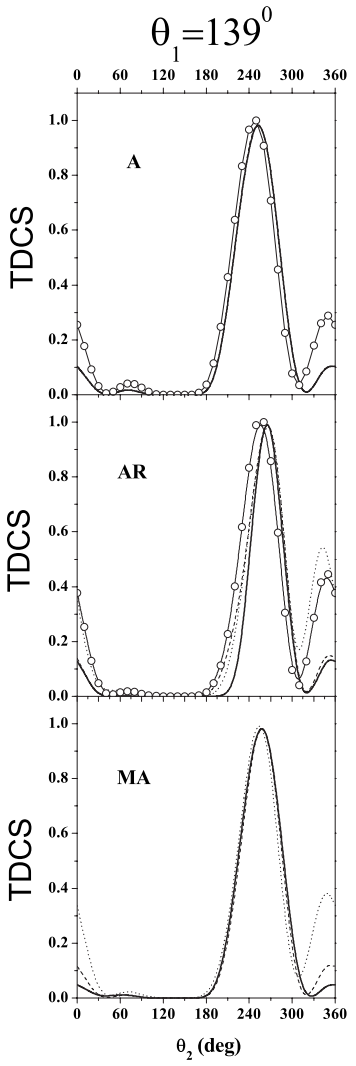


FIG. 2. Threefold differential cross section (TDCS) for $(\gamma,2e)$ ionization of the helium ground state, as a function of the angle of one of the ejected electrons $\theta_2$, with $\theta_1=139°$; the polarization vector is held fixed at 0°. The incident electron is at ~5.6 keV and the two ejected electrons escape with equal energy (10 eV). The calculated TDCSs, normalized to one at the maximum, are obtained in the velocity gauge with the C3 final state and several initial state wave functions: top panel, *A* functions; middle panel, AR functions; and bottom panel, MA functions. In all panels, functions with polynomial behavior are plotted with solid lines, those with exponentially decreasing behavior with dashed lines, those with exponentially increasing behavior with dotted lines, and with oscillatory conditions with solid lines with open circles.

smaller when compared to those found with AR and MA wave functions (see below).

#### 2. $\psi_i$ with angular and radial correlation (*AR*)

If one now includes both radial and angular correlation through a configuration interaction approach, the picture changes substantially. The four AR selected functions have a much better mean energy than the *A* functions and can be considered as of intermediate quality. However, when used for calculating $(e,3e)$ cross sections, no agreement is observed with experimental data (Fig. 1), no matter what functional form is used. Not only the magnitude, but also the shapes are lost. The enhancement of the cross sections at $\theta_2$ in the direction $\theta_1$-$\pi$ is directly related to the presence of the $1s2s+2s1s$ term. Interference between the contributions to the matrix element $T_{fi}$ yields these important shape modifications. As more configuration terms are included in the initial state, these interferences cancel out and the cross sections become progressively similar to the MA ones. It should be also pointed out that the use of oscillating functions (*Os*) through the Pluvinage-basis functions has particularly dra-

TABLE II. Gauge discrepancies ratios for $(\gamma,2e)$ processes, computed at the maximum of the TDCS for $\theta_1=139°$.

| Trial function | Equation | $L/V$ | $L/A$ |
|---|---|---|---|
| $\Psi^{A,P}$ | (7) | 9.06 | 19.29 |
| $\Psi^{A,e-}$ | (8) | 9.11 | 19.50 |
| $\Psi^{A,e+}$ | (9) | 9.17 | 19.63 |
| $\Psi^{A,Os}$ | (10) | 8.26 | 22.77 |
| $\Psi^{AR,P}$ | (11) | 35.73 | 195.57 |
| $\Psi^{AR,e-}$ | (12) | 22.64 | 69.17 |
| $\Psi^{AR,e+}$ | (13) | 24.67 | 136.61 |
| $\Psi^{AR,Os}$ | (14) | 10.35 | 43.45 |
| $\Psi^{MA,P}$ | (15) | 10.92 | 28.94 |
| $\Psi^{MA,e-}$ | (16) | 7.42 | 42.48 |
| $\Psi^{MA,e+}$ | (17) | 6.67 | 44.05 |

matic effects. This has been observed also with other Pluvinage-type trial wave functions [19,22].

Gauge discrepancies for $(\gamma,2e)$ are more important with the four AR trial wave functions than for the $A$ initial bound states (see Table II). In Fig. 2 we observe that (i) the main peak of the cross sections is slightly shifted when compared to the $A$ results; (ii) the oscillatory function gives a relatively bigger secondary peak, similarly to that observed in the $A$ case; and (iii) the shapes depend more on the functional form of the correlation factors, similarly to that observed for $(e,3e)$ in Fig. 1. Moreover, with AR initial states, important differences can be seen (not shown here) when comparing the differential cross sections on an absolute scale.

In view of the (improved) values of the ground state energy and other mean values (see Table I), the AR correlated trial wave functions should be considered as better than the $A$ ones. However, when combined with the C3 final state, they yield poorer $(e,3e)$ cross sections [and more fluctuations in $(\gamma,2e)$ TDCSs]. The reason can be possibly related to the fact that the initial and final states are not described in a balanced way. In this case, thus, the ground initial state mean energy does not seem to be a relevant indicator. A configuration interaction construction similar to the one used for the initial channel should be implemented for the final channel using an approach similar to the one described in Ref. [35]; this, however, is a difficult task and far beyond the main scope of the present work.

#### 3. $\psi_i$ with angular and radial correlation (MA)

With the more advanced trial wave functions considered in Sec. II D 3, the mean energy and other mean quantities are getting closer to the numerically exact ones. One would expect a better agreement for both double ionization processes.

For $(e,3e)$ processes, these advanced wave functions manage to get the FDCS shapes correctly but not the magnitude (about a factor of 1.5–2 too large depending on the $\theta_1$ angle), and this independently of the functional form. Other bound wave functions with even better energies have been considered. Whether they satisfy the Kato cusp conditions [32] exactly [36], almost exactly [20], or not at all (like Kinoshita [6] or Bonham and Kohl [29] wave functions, see [18,26]), practically the same cross sections were found.

As the $(\gamma,2e)$ calculations are concerned, the MA functions surprisingly yield larger gauge discrepancies than with the simpler wave functions $(A)$, but generally smaller than those found with the AR functions (see Table II). The shapes of the TDCSs are similar to each other (little functional dependence), and the main peak is situated at approximately the same $\theta_2$ angle as for AR functions.

The analysis of all the results given above seem to indicate that initial wave functions which contain angular correlation only ($A$ functions), when combined with the C3 double continuum, are more adequate to describe the high incident energy $(e,3e)$ processes with two electrons escaping at 10 eV. The fact that they yield a relatively bad ground state mean energy is not significant. Jones and Madison [17] suggested that, in the case of Pluvinage function, this may be related to the fact that this function diagonalizes the Hamiltonian, and hence gives a balanced description of initial and final states. From the above analysis, and as already stated in [18], $A$ functions which do not diagonalize the Hamiltonian yield practically the same result; this is true whatever the functional form of the correlation factor. It can thus be stated that, for the $(e,3e)$ processes under scrutiny here, the asymptotic $r_{12}$ behavior does not play any role. The fact that initial and final states have a similar structure, and hence satisfy similar parts of the full three-body Hamiltonian, is clearly responsible for the relatively minor gauge discrepancy values observed in Table II for $(\gamma,2e)$ processes.

A comment on the role of cusp conditions further completes the investigation. All initial states considered above satisfy exactly all two-body cusp conditions. Several other trial bound wave functions, not satisfying one or more of these conditions, have been used in conjunction with the double continuum C3 description. In [18], an $A$ function not satisfying the electron-electron coalescence condition was used to demonstrate that practically the same result as other $A$-type functions is found; similarly, MA functions not fulfilling any of the conditions yield practically the same cross sections [18,20] as those shown here. Hence it can be concluded that, when combined with the C3 final state, whether the initial state satisfies or not Kato cusp conditions does not matter in these high incident energy $(e,3e)$ processes. This can be related to what is known from studies of photo-double ionization for which the cusp conditions have fundamental importance at high energy regimes [38] (the electron-nucleus and electron-electron cusp condition playing a role at different energy regimes). For two electrons ejected with relatively low energy (10 eV) in a $(\gamma,2e)$ process, and thus similarly in a $(e,3e)$ process, we do not expect the electron-electron cusp behavior to play a crucial role.

It emerges thus that the behavior of the ground state wave function near the two-body coalescence points, or at large $r_{12}$ values has little influence on, the C3 calculated cross sections. The description of the wave functions involved in the regions of the configuration space where the three interparticle distances take intermediate values seem to be the most important for the $(e,3e)$ processes under scrutiny.

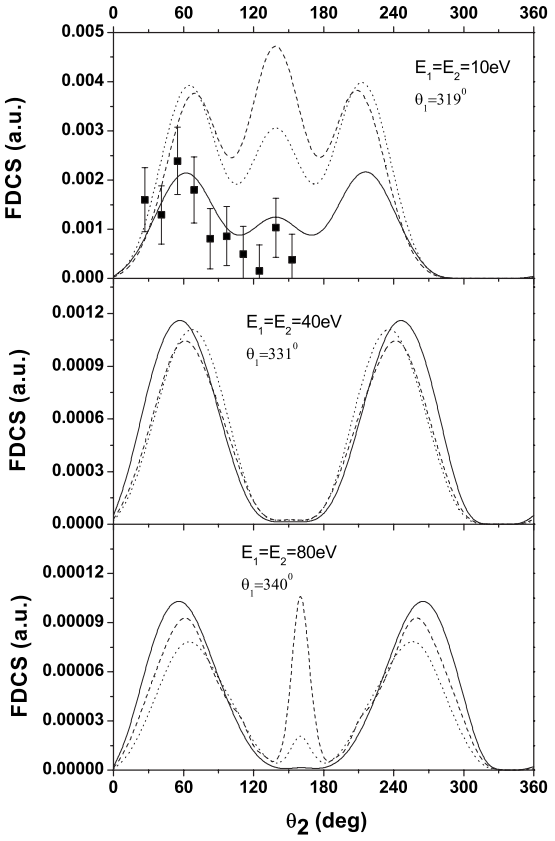


FIG. 3. Fivefold differential cross section (FDCS) for $(e,3e)$ ionization of the helium ground state, as a function of the angle of one of the ejected electrons $\theta_2$, with $\theta_1$ fixed in the direction of the momentum transfer as indicated. The incident electron (at ~5.6 keV) is scattered at 0.45°. The two ejected electrons escape with equal energy $E_1=E_2$ of 10 eV (top panel), 40 eV (middle panel), and 80 eV (bottom panel). The absolute experimental data [11]: full squares. The calculated FDCSs are obtained with the C3 final state and the $\Psi^{A,e-}$ (solid lines), $\Psi^{AR,e-}$ (dashed lines), and $\Psi^{MA,e-}$ (dotted lines) wave functions.

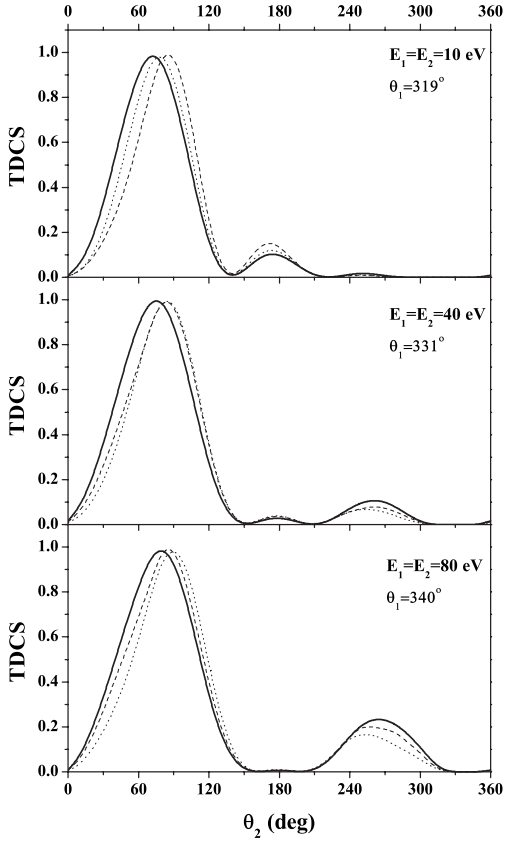


FIG. 4. Same as for Fig. 3 but for the threefold differential cross section (TDCS), normalized to 1 at the maximum, for $(\gamma,2e)$ ionization in the velocity gauge. The polarization vector is held fixed at 0°.

### B. Ejected energy dependence

We now perform a similar study but varying the energy $E_1=E_2$ of the two ejected electrons (the incident energy is fixed at 5.6 keV). One should keep in mind that we expect the final state to be better described by the C3 double continuum if the ejected electrons escape with higher energy. In Fig. 3 we show the $(e,3e)$ results obtained for $E_1=E_2=10$, 40, and 80 eV calculated for $\theta_1$ fixed in the direction of the momentum transfer ($\theta_1=319°$, 331°, and 340°, respectively). In each panel we have plotted the FDCSs obtained with three different initial states, one representative of each class; functions $\Psi^{A,e-}$ (*A*), $\Psi^{AR,e-}$ (AR), and $\Psi^{MA,e-}$ (MA). At 10 eV we have included the experimental data of [11]. As the ejected energies increase the cross sections magnitude decreases. Three major observations can be made. First, whatever the ejected energies, the FDCS shapes obtained with the *A* and MA wave functions are always similar; the AR cross sections, on the other hand, show some changes in shapes linked to the $1s2s+2s1s$ presence (as seen in Fig. 3 for 10 and 80 eV). Second, when the ejected energy is $E_1=E_2=40$ eV, all results are very similar in magnitude independently of the initial state used in the calculation. Third, when the ejected energy is increased an inversion of magnitude takes place; while at $E_1=E_2=10$ eV the MA cross sections are a factor of 2 higher than the *A* result (see Sec. III A), almost no difference is noticed at $E_1=E_2=40$ eV, and the ratio is inverted (about 0.75) at $E_1=E_2=80$ eV. This dependence on the ejected energy leads to the following statement: if the $(e,3e)$ experiment had been performed with $E_1=E_2=40$ eV, no substantial difference between the FDCSs calculated with several initial states (in combination with the C3 double continuum) would have been observed.

Let us now turn to $(\gamma,2e)$ processes. The gauge discrepancies persist for higher ejected electrons energies. Figure 4 shows the TDCSs obtained in the velocity gauge with the same initial wave functions and at the same ejected energies as in Fig. 3. For all initial states, the differences in TDCSs remain as the energy increases reflecting the differences in the interelectronic correlation included in each function. Overall, the $A/V$ ratio increases while $V/L$ decreases for increasing energies; however the $V/L$ ratio is more sensitive to the differences among the initial states.

To further illustrate the energy dependence we have considered ejected energies from $E_1=E_2=5$ eV up to 100 eV. For each energy, and for $\theta_1$ in the direction of the corresponding momentum transfer, we have calculated FDCSs for

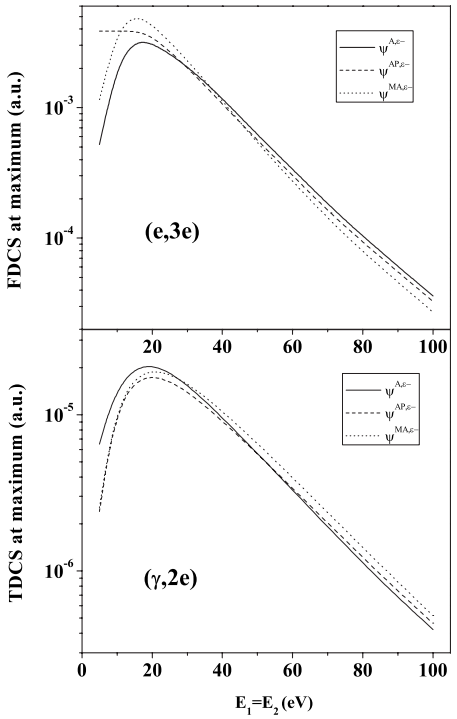


FIG. 5. The maximum of the FDCS for $(e,3e)$ and of the TDCS for $(\gamma,2e)$ as a function of the ejected energy $E_1=E_2$, calculated with the C3 final state and the $\Psi^{A,e-}$ (solid line), $\Psi^{AR,e-}$ (dashed lines), and $\Psi^{MA,e-}$ (dotted lines) wave functions.

$(e,3e)$ and TDCSs in the velocity gauge for $(\gamma,2e)$, again with initial wave functions $\Psi^{A,e-}$ $(A)$, $\Psi^{AR,e-}$ (AR), and $\Psi^{MA,e-}$ (MA). For each energy, the shapes of the FDCSs are similar for the $A$ and MA functions, as observed in Fig. 1 for $E_1=E_2=10$ eV. Because of the choice of $\theta_1$ , the FDCSs present a symmetry with respect to $\theta_2=-\theta_1$. In Fig. 5 (top panel) we have represented as a function of the ejected energy $E_1=E_2$, the value of the (symmetric) maximum of the $(e,3e)$ FDCSs. It clearly appears that, for $E_1=E_2<35$ eV, the use of an $A$ function yields results lower than those found with a MA initial state, while the reverse is true for $E_1=E_2>35$ eV. The AR results are somewhere in between, and the three curves cross each other approximately at 35 eV. A similar pattern is observed for $(\gamma,2e)$ processes (bottom panel of Fig. 5) for which the (main) maximum of the TDCSs also exhibits a crossing of the $A$ and MA results at about $E_1=E_2=35$ eV. Besides, the AR result somehow is slightly different, and crosses the MA result at a higher ejected energy, around $E_1=E_2=50$ eV. Overall, for both $(e,3e)$ and $(\gamma,2e)$ processes there is a change in the relative magnitude of the differential cross sections computed with different initial states.

## IV. SUMMARY AND PERSPECTIVES

We have performed a systematic study of double ionization processes of the helium ground state by high energy electron and photon impact. The two escaping electrons are described by the C3 double continuum wave function, and several initial bound states satisfying the two-body cusp conditions have been considered. The computed cross sections are quite sensitive to the amount of correlation included in the bound wave function.

From the analysis of the calculated cross sections at ejected energies of $E_1=E_2=10$ eV, and the comparison with the absolute experimental $(e,3e)$ data [11], it emerges that: (i) bound wave functions with only angular correlation seem better suited for $(e,3e)$; however, since gauge discrepancies exist for $(\gamma,2e)$, these initial states cannot be considered as well-balanced with respect to the final state C3 description; and (ii) intermediate quality or more advanced bound wave functions (which include both radial and angular correlation) yield a better ground state energy and other mean values, but are even less balanced with respect to the C3 wave function. Hence while these mean values are quality indicators of the initial wave function, they do not yield an improvement of collision cross sections: magnitude (and even shape in the AR case) disagreement for $(e,3e)$ processes. Gauge discrepancies and magnitude differences for $(\gamma,2e)$ are observed, in particular for AR initial states. Hence it can be concluded that, whatever the chosen initial state trial wave function—satisfying or not Kato cusp conditions, and with different asymptotic behaviors—the C3 function is not suitable to describe sufficiently well the double continuum of two electron ejected at 10 eV. The $(e,3e)$ agreement obtained with $A$ functions can thus be considered as fortuitous. It should be reminded, though, that none of the theoretical models mentioned in the Introduction are satisfactory for both $(e,3e)$ and $(\gamma,2e)$ processes, so the study of these differential double ionization processes cannot be considered as resolved from a theoretical point of view.

By varying the ejected energy, our $(e,3e)$ calculated cross sections with the C3 final state show that: (i) for about $E_1=E_2=35$ eV, the calculated cross sections do not depend much on the initial wave function; and (ii) at lower energies the simpler wave functions $(A)$ yield lower results than highly correlated ones (MA), while the reverse is true at energies higher than 35 eV. Hence the observations made on the comparison at 10 eV do not necessarily hold at other ejected energies. A similar trend holds true also for the $(\gamma,2e)$ case. The fact that simple wave functions $(A)$ in combination with the double continuum C3 wave function yield a good agreement with the experiments at $E_1=E_2=10$ eV has then to be considered a fortuitous coincidence.

In view of the present findings, it would be very useful to have new absolute experimental $(e,3e)$ data in the same high incident energy regime but with higher ejected energy values. In particular, it would be interesting to have a measurement at about $E_1=E_2=35$ eV since the use of several initial states predict the same cross sections; if experiment–theory disagreement would be observed, it should then be associated only to a poor description of the final state by the double continuum C3 wave function. A measurement at a higher energy, say at $E_1=E_2=80$ eV, would also be very useful since it would confirm that the agreement observed at 10 eV with $A$ functions is fortuitous. While the cross section at ejected energies of 35 eV is of the same order of magnitude $(10^{-3}$ a.u.) as at 10 eV, the measurement at 80 eV would be experimentally more difficult as the maximum is one order of magnitude smaller.

From a theoretical point of view, it would also be interesting to see if other models such as the CCC approach show the same behavior as a function of the ejected energy. We should remind that this theory, which according to the authors uses nearly exact final state wave functions, fails to reproduce the magnitude of the $(e,3e)$ cross sections whatever the initial state considered [12,13].

The present study leads to an additional conclusion: collisional processes cannot be easily used as a conclusive test for the quality of approximated wave functions. As shown here, different conclusions are obtained when approximate initial and final states are used for different double ionization processes, and furthermore they are energy dependent. It would therefore be interesting and useful to have an absolute test which indicates whether a given trial wave function, in particular the double continuum, can be considered as good, and this independently of the collision process.

## ACKNOWLEDGMENTS

We are grateful to Azzedine Lahmam-Bennani for his valuable and constructive comments on the manuscript. F. D. C. would like to acknowledge the financial support of ANPCYT (Grant No. PICT 04/20548) and Conicet (Grant No. PICT 5595). G. G. would like to acknowledge the support by PICTR Grant No. 03/0437 of the ANPCYT (Argentina) and Grant No. PGI 24/F038 of the Universidad Nacional del Sur (Argentina).

[1] J. Berakdar, A. Lahmam-Bennani, and C. Dal Cappello, Phys. Rep. **374**, 91 (2003).
[2] J. S. Briggs and V. Schmidt, J. Phys. B **33**, R1 (2000).
[3] B. H. Bransden and C. J. Joachain, *Physics of Atoms and Molecules*, 2nd ed. (Prentice-Hall, Englewood Cliffs, NJ, 2003).
[4] S. P. Lucey, J. Rasch, C. T. Whelan, and H. R. J. Walters, J. Phys. B **31**, 1237 (1998).
[5] C. R. Garibotti and J. E. Miraglia, Phys. Rev. A **21**, 572 (1980); M. Brauner, J. Briggs, and H. Klar, J. Phys. B **22**, 2265 (1989).
[6] T. Kinoshita, Phys. Rev. **105**, 1490 (1957).
[7] S. Otranto and C. R. Garibotti, Eur. Phys. J. D **21**, 285 (2002).
[8] S. Otranto and C. R. Garibotti, Eur. Phys. J. D **27**, 215 (2003).
[9] L. Avaldi and A. Huetz, J. Phys. B **38**, S861 (2005).
[10] A. S. Kheifets and I. Bray, Phys. Rev. A **58**, 4501 (1998).
[11] A. Lahmam-Bennani, I. Taouil, A. Duguet, M. Lecas, L. Avaldi, and J. Berakdar, Phys. Rev. A **59**, 3548 (1999).
[12] A. S. Kheifets *et al.*, J. Phys. B **32**, 5047 (1999).
[13] A. S. Kheifets and I. Bray, Phys. Rev. A **69**, 050701(R) (2004).
[14] S. A. Zaytsev, V. A. Knyr, and Yu. V. Popov, Phys. At. Nucl. **70**, 676 (2007).
[15] V. A. Knyr, V. V. Nasyrov, and Yu. V. Popov, in *Correlation and Polarization in Photonic, Electronic, and Atomic Collisions*, edited by G. F. Hanne *et al.*, AIP Conf. Proc. No. 697 (AIP, Melville, NY, 2003), p.76.
[16] V. V. Serov, V. L. Derbov, B. B. Joulakian, and S. I. Vinitsky, Phys. Rev. A **75**, 012715 (2007).
[17] S. Jones and D. H. Madison, Phys. Rev. Lett. **91**, 073201 (2003).
[18] L. U. Ancarani, T. Montagnese, and C. Dal Cappello, Phys. Rev. A **70**, 012711 (2004).
[19] S. Jones, J. H. Macek, and D. H. Madison, Phys. Rev. A **70**, 012712 (2004).
[20] O. Chuluunbaatar, I. V. Puzynin, P. S. Vinitsky, Y. V. Popov, K. A. Kouzakov, and C. Dal Cappello, Phys. Rev. A **74**, 014703 (2006).
[21] F. D. Colavecchia, G. Gasaneo, and K. V. Rodriguez, J. Electron Spectrosc. Relat. Phenom. **161**, 73 (2007).
[22] L. U. Ancarani and C. Dal Cappello, J. Electron Spectrosc. Relat. Phenom. **161**, 22 (2007).
[23] G. Gasaneo, S. Otranto, and K. V. Rodriguez, *Proceedings of the XXIV International Conference on Photonic, Electronic and Atomic Collision* (World Scientific, Singapore, 2006), p. 360.
[24] L. U. Ancarani, C. Dal Cappello, and T. Montagnese, in *Ionization, Correlation, and Polarization in Atomic Collisions*, edited by A. Lahmam-Bennani and B. Lohmann, AIP Conf. Proc. No. 811 (AIP, Melville, NY, 2006), p.1.
[25] A. S. Kheifets, Phys. Rev. A **69**, 032712 (2004).
[26] L. U. Ancarani, T. Montagnese, and C. Dal Cappello, in *Electron and Photon Impact Ionization and Related Topics*, edited by B. Piraux, IOP Conf. Proc. No. 183 (Institute of Physics, London, 2005), p. 21.
[27] C. Le Sech, J. Phys. B **30**, L47 (1997).
[28] P. Pluvinage, Ann. Phys. **5**, 145 (1950); J. Phys. Radium **12**, 789 (1951).
[29] R. A. Bonham and D. A. Kohl, J. Chem. Phys. **45**, 2471 (1966).
[30] L. U. Ancarani and G. Gasaneo, Phys. Rev. A **75**, 032706 (2007).
[31] J. H. Macek and S. Jones, Radiat. Phys. Chem. **75**, 2206 (2006).
[32] T. Kato, Commun. Pure Appl. Math. **10**, 151 (1957).
[33] G. Gasaneo, F. D. Colavecchia, C. R. Garibotti, J. E. Miraglia, and P. Macri, Phys. Rev. A **55**, 2809 (1997).
[34] P. A. Macri, J. E. Miraglia, C. R. Garibotti, F. D. Colavecchia, and G. Gasaneo, Phys. Rev. A **55**, 3518 (1997).
[35] G. Gasaneo and L. U. Ancarani, Phys. Rev. A **77**, 012705 (2008).
[36] K. V. Rodriguez, G. Gasaneo, and D. M. Mitnik, J. Phys. B **40**, 3923 (2007).
[37] G. W. F. Drake, *Springer Handbook of Atomic, Molecular, and Optical Physics* (Springer, New York, 2005).
[38] T. Suric, E. G. Drukarev, and R. H. Pratt, Phys. Rev. A **67**, 022709 (2003).